Clays Clay Miner., Vol. 70, No. 4:527–538, 2022
https://doi.org/10.1007/s42860-022-00200-w

ORIGINAL PAPER

Preparation and Antibacterial Properties of Carvacrol-loaded Composite Microcapsules via Palygorskite-Stabilized Pickering Emulsions

Aiping Hui · Yongfeng Zhu · Fangfang Yang · Yuru Kang · Aiqin Wang

Accepted: 17 August 2022 / Published online: 6 September 2022

Abstract Essential oils (including carvacrol, CAR) have been used in the medicinal and health field because of their broad-spectrum antibacterial activities. However, the volatility and pungent odor are still the greatest obstacles to wider application. The purpose of the present study was to address those problems by encapsulating the antibacterial CAR in palygorskite (Plg) by integrating it into Pickering emulsions with complex coacervation. The CAR in Pickering emulsion was formed firstly by stabilization with the CAR-modified Plg; then, the emulsion droplets were embedded and fixed in the microcapsule through the subsequent complex coacervation process, which occurred between the quaternary ammonium salt of chitooligosaccharides (HACC) and sodium alginate (SA) via calcium ions. The microcapsules obtained were characterized by Fourier-transform infrared spectroscopy (FTIR), scanning electron microscopy (SEM), and thermogravimetric analysis (TGA). The results demonstrated that the microcapsules presented a nearly sphere-like shape with a mean diameter of 3.5 mm but had a porous interior structure. The Plg plays multiple roles in the preparation process, including increasing the emulsion stability, improving the encapsulation efficiency of CAR, and the thermostability of microcapsules. The microcapsules showed remarkable antibacterial properties against *Escherichia coli* (*E. coli*) and *Staphylococcus aureus* (*S. aureus*), and inhibition rates toward *E. coli* and *S. aureus* reached 100% when the microcapsules were encapsulated with 15 or 20% of CAR, respectively. The microcapsules obtained could be used as antibacterial agents in food preservatives, animal feed, and other health-related consumer products.

Keywords Antibacterial properties · Carvacrol · Microcapsules · Palygorskite · Pickering emulsions

Associate Editor: Lynda B. Williams

A. Hui · Y. Zhu · F. Yang · Y. Kang · A. Wang (✉)
Key Laboratory of Clay Mineral Applied Research of Gansu Province, Center of Eco-material and Green Chemistry, Lanzhou Institute of Chemical Physics, Chinese Academy of Sciences, Lanzhou 730000, People's Republic of China
e-mail: aqwang@licp.cas.cn

Introduction

Essential oils have been used for thousands of years in the medicinal and health field in ancient Egypt, Greece, India, and China because of their broad-spectrum antibacterial activities (Issouffou et al., 2018; Sharifi-Rad et al., 2018; Shi et al., 2018; Vel et al., 2017). For instance, cinnamon essential oil could reduce the viability of *Escherichia coli (E. coli)*, *Salmonella typhimurium*, *Staphylococcus aureus,* and *Vibrio parahaemolyticus* (Chuesiang et al., 2021). Origanum oil, thyme oil, and citrus aurantium bergamia fruit oil can inhibit food-borne pathogens, including *E. coli*, *Salmonella*, *Bacillus cereus*, *Aspergillus flavus*, and drug-resistant microbial strains (Sharifi-Rad et al., 2018; Tariq et al., 2019). Nowadays, essential oils are applied as antibiotics and are still used in pharmaceuticals, cosmetics, foods, and agriculture (Alkan Tas et al., 2019; Tariq et al., 2019).

The antibacterial performance of essential oils derives from their main active component, e.g. carvacrol

(CAR), which is the main constituent in thyme and oregano. CAR has been verified to show much greater antibacterial activities than those of other compounds present in essential oils due to the structural free hydroxyl group, hydrophobicity, and a phenol component (Ryu et al., 2019). Until now, CAR has been used as a natural preservative in the food industry, or as a feed additive to reduce aflatoxin contamination in poultry feed (Yin et al., 2015). Several shortcomings of CAR, including significant volatility, poor water solubility, its pungent odor, and its unstable chemical structure in air, light, and high temperature, are still the greatest obstacles to wider application (Ryu et al., 2019; Yildiz et al., 2018). Many efforts have been made to overcome these weaknesses, including encapsulation of CAR into emulsions, nanoemulsions, nanoliposomes, microcapsules, films, and nanocarriers (Bahrami et al., 2020). Among them, the encapsulation of CAR into microcapsules via complex coacervation is a popular and efficient strategy, because of its low cost, convenient operation, high encapsulation efficiency, reduced wall permeability, and prolonged release time (Bakry et al., 2019; Chen et al., 2016; Dong et al., 2011; Muhoza et al., 2019; Timilsena et al., 2017; Yang et al., 2014; Yang et al., 2015). Interestingly, if the essential oil is divided into smaller droplets and encapsulated into the separated "sub-box" of coacervate microcapsules, the slow-release performance is enhanced, even if the microcapsules have been damaged.

The best method for encapsulation of CAR into coacervate microcapsules is by integrating an emulsion and complex coacervation technique. Due to the poor stability of conventional emulsions, in comparison, Pickering emulsions stabilized by solid particles instead of surfactants show an increased barrier effect, because the particles adsorb irreversibly at the oil–water interface and form a rigid shell (Cai et al., 2019; Li et al., 2021a, b; Lu et al., 2014; Pickering, 1907; Ramsden, 1903). More importantly, the stabilized particles could be incorporated into the matrix of microcapsules with increased compactness and strength. Therefore, various effects will increase the encapsulation efficiency of essential oils and prolong their shelf lives. Recent research has also found that the shape of particles has a significant effect on the adsorption behavior of the oil–water interface, and particles with rod-shaped or tube-like morphology display greater stability than spherical particles (Lu et al., 2020; Wang et al., 2022). This suggests that the clay minerals increase the stability of Pickering emulsions. Palygorskite (Plg), a natural, rod-like, hydrated magnesium aluminum silicate mineral, typically exhibits crystal lengths of 1–5 μm and has been used widely in the stabilization of Pickering emulsions (Kretz, 1983; Li et al., 2021a, b; Marosz et al., 2020; Wang et al., 2015). Moreover, due to the large specific surface area and the abundant active adsorption sites, the external surface property of Plg is easily modified and adjusted by adsorbing small organic molecules or polymers (Blanco et al., 1988; Kang et al., 2022; Lu et al., 2020).

The objective of the current study was to use Plg to develop a novel and effective method to encapsulate volatile oils such as CAR into the 'sub-box' by integrating Pickering emulsions with complex coacervation. The hypothesis was that the morphology, particle size, and thermal stability of the microcapsules could be optimized using Plg to obtain the greatest loading capacity, encapsulation efficiency, and antibacterial properties of CAR, in preparation for extensive applications in food, poultry feed, and health-related consumer products.

Materials and Methods

Materials

Carvacrol (CAR, 99%) was purchased from Macklin Biochemical Co., Ltd. (Shanghai, China). Non-ionic surfactant, Span 80 (Sorbitan Monooleate, $C_{24}H_{44}O_6$, analytical reagent [AR] grade), was purchased from the National Medicines Co., Ltd. (Shanghai, China). Anhydrous calcium chloride (≥96%) was provided by Kermel Chemical Regent Co., Ltd. (Tianjin, China). Sodium alginate (SA, AR grade) was supplied by Xilong Scientific Co., Ltd. (Guangzhou, China). Quaternary ammonium salt of chitooligosaccharides (HACC, ≥90%) was purchased from Jiaxing Korui Biotech Co., Ltd. (Jiangsu, China) and palygorskite was provided by Huida Mineral Technology Co., Ltd. (Jiangsu, China). Acid treatment of Plg was by 4% HCl solution with a solid/liquid ratio (w/w) of 1:10 to remove the associated carbonates, then it was filtered with a 200-mesh sieve. The chemical composition was: SiO_2, 50.18; Al_2O_3, 11.15, MgO, 4.21; Fe_2O_3, 9.37; Na_2O, 5.92; K_2O, 2.03, and CaO, 1.37%, and an SEM image is shown in the Supplementary Material (Fig. S1 in Supplementary Materials). Other chemicals were used directly without further purification.

https://doi.org/10.1007/s42860-022-00200-w Published online by Cambridge University Press

Preparation of CAR Microcapsules

Plg-stabilized Pickering emulsion was prepared by a simple process. Typically, a 2 wt.% Plg aqueous suspension was used to optimize various amounts of CAR (2.5, 5, 7.5, and 10 g, which were 5, 10, 15, and 20% with respect to the weight of the water, respectively) and stirred at 200 rpm for 1 h. Then, 50 mL of SA solution (1% w/w) containing 0.5% of Span 80 was added, and the dispersion was stirred at 8000 rpm for 10 min to form an homogeneous Pickering emulsion. After that, 10 mL of HACC solution (10% w/w) was added to the emulsion and stirred for an additional 10 min. Then, the emulsion was added dropwise to a $CaCl_2$ solution (1% w/w) by a peristaltic pump under stirring at 160 rpm. The microcapsules obtained were dried at 37°C for 12 h. In order to optimize the preparation parameters of microcapsules, various amounts of Plg (4, 6, 8, and 10% with respect to the weight of the water) were tested to optimize the preparation parameters based on loading capacity and encapsulation efficiency, and the emulsion obtained was labeled as a Plg-stabilized Pickering emulsion. As a comparison, the microcapsules constructed with the conventional emulsion integrated with complex coacervation were also prepared as the above steps. The conventional emulsion was formed as: 15% of CAR dispersed into 50 mL SA solution (1% w/w) containing 1% of Span 80.

Characterization

The chemical composition of Plg was analyzed using a Minipal 4 X-ray fluorescence spectrometer (PANalytical Co., Almelo, The Netherlands). The digital photographs of Pickering emulsions were taken with a Nikon D600 digital camera (D600, Nikon, Tokyo, Japan), and the Pickering emulsion was observed using an industrial digital camera (DYF-1600, Shanghai, China). The morphology and microstructure of CAR microcapsules were observed by scanning electron microscopy (SEM, JSM-5600LV, JEOL, Tokyo, Japan). The structure of the microcapsules prepared as KBr pellets was characterized using an FTIR spectrometer (Nicolet Nexus iS50, Thermo Scientific, Waltham, Massachusetts, USA) over the range 4000–400 cm^{-1}. The thermal stability of the microcapsules was evaluated by thermal gravimetric analysis (TGA) (STA6000, PerkinElmer, Waltham, Massachusetts, USA) over the range 50–750°C in a pure oxygen atmosphere with a heating rate of 10°C/min. The hydrophilic and hydrophobic performance of the Plg surface was tested with a Contact Angle System (DSA100S, Kruss, Germany) equipped with a tilting table, and the powder was pressed into sheets at a tableting pressure of 2–4 MPa. The syringe was positioned in a way that the water drop (2 μL) contacted the surface of the sheet before leaving the needle.

Loading Capacity (LC) and Encapsulation Efficiency (EE)

The LC and EE were applied to optimize the amounts of CAR and Plg by the following method: CAR microcapsules were added to a sealed conical flask containing 50 mL of absolute ethyl alcohol and treated for 2 h in a sonic bath, and then shaken at 37°C for 24 h. After that, the supernatant was separated by centrifugation. The concentration of CAR was determined with the ultraviolet-visible spectrophotometer at 276 nm. This test was repeated three times and the mean values of the samples were calculated according to the standard curve. The LC and EE were calculated according to the following equations, respectively.

$$\mathrm{LC} = M_t/M_m \times 100\% \quad (1)$$

$$\mathrm{EE} = M_t/M_0 \times 100\% \quad (2)$$

where M_m and M_t were the weight of microcapsules and measured CAR, respectively, and M_0 was the weight of initial amount of CAR.

Antibacterial Test

The antibacterial properties of CAR microcapsules were assessed by the traditional plating method against Gram negative *E. coli* (ATCC 25922) and Gram positive *S. aureus* (ATCC 25923), which were kindly provided by the Laboratory Medicine Center of Lanzhou University Second Hospital. The bacteria were cultivated aseptically in Luria-Bertani (LB) nutrient broth at 37°C while shaking at 160 rpm for 12 h, bacterial inocula were diluted to 0.5 MCF units (10^8 CFU/mL) using phosphate buffers, and then 100 μL of the broth was taken out and added to 900 μL of LB medium for culturing in a 37°C shaker incubator at 160 rpm for 3 h to reach the exponential growth phase (10^7 CFU/mL). The steps were repeated to obtain fresh bacteria in

suspension (10^5 CFU/mL), then 5 mL of bacterial suspension (10^5 CFU/mL) was transferred to a glass centrifuge tube containing 50 mg of the test sample. The tube was placed on an orbital shaker at 160 rpm for 24 h. Later, 1 mL of the treated bacterial suspension was plated on an agar plate and kept in a microbiological incubator at 37°C in a >95% humidified atmosphere with 5% CO_2 for 24 h. Finally, the number of colony forming units (CFU) was counted by visual inspection to calculate the inhibition rate (IR), using the following equation (Ma et al., 2013):

$$IR = (N_0 – N_t)/N_0 \times 100\% \quad (3)$$

where, N_0 and N_t are the number of *E. coli* or *S. aureus* colonies without treatment and treated with microcapsules for 24 h, respectively. To evaluate the antibacterial properties of CAR microcapsules, the bacterial suspensions acted as a blank control and the microcapsules without CAR as a positive control.

In order to compare the bacterial killing effect between the microcapsules and CAR, the agar plate experiments for *E. coli* and *S. aureus* were also tested with different amounts of pure CAR, in which the bacterial suspension was also 10^5 CFU/mL. Other steps were the same as above and the inhibition rate (%) was calculated by Eq. 3.

Results and Discussion

Formation of Plg-stabilized Pickering Emulsions

The use of Plg in the preparation of Pickering emulsions has been reported in several studies (e.g. Lu et al., 2014). However, due to inherently strong hydrophilicity, the Plg needs to be modified and its surface performance adjusted. Because of its sufficiently active silicon hydroxyl and porous structure, Plg can be modified easily using cetyltrimethylammonium bromide, chitooligosaccharides, and γ-methacryloxypropyl trimethoxysilane (Hui et al., 2020; Pan & Liu, 2021; Wang et al., 2022). The Plg also shows favorable adsorption performance for essential oil molecules, therefore, the amphipathicity of Plg can be adjusted directly by the absorption of CAR. The contact angle, which reflects the surface amphipathicity of Plg was increased by mixing Plg with increasing amounts of CAR (Fig. 1a–f and Fig. S2), and then reached steady-state as the concentration of CAR exceeded 20% (Fig. 1g). In addition, the contact angle of Plg adsorbed with CAR after immersing with *n*-hexane for 4 h was still larger than that of the original Plg (Fig. S3), suggesting that CAR molecules were adsorbed onto the Plg surface or entered the channel in Plg through hydrogen-bond interactions between the phenolic hydroxyl group of CAR and silanol of Plg (Fig. 1h) (Zhong et al., 2020, 2021).

When the SA solution was added to the mixture of Plg and CAR, the Pickering emulsion eventually turned milky white after rapid stirring. The emulsion diffused through water, but was retained in oil, indicating that the oil-in-water Pickering emulsions had been prepared successfully (Fig. S4). Note that the emulsions can only be formed by initially mixing the CAR and Plg. If Plg is mixed with CAR by dropping CAR into the Plg dispersion, this indicates that Plg may preferentially adsorb water, so that CAR cannot be adsorbed to the Plg. The optical microscopy of Pickering emulsions prepared with different amounts of Plg and CAR showed the trend that the size of emulsion droplets decreased with the increase of CAR concentration (Fig. 2a–d). This is because the increase in CAR is beneficial to modification of Plg, and an emulsion with smaller droplets can be obtained (Fig. 2d). Besides, some CAR may diffuse into the oil–water interface and have a positive effect on the stability of the emulsions. The same phenomenon was also observed as the droplet size decreased gradually with increasing Plg content (Fig. 2e–h), because modified Plg will generate better stabilization for emulsion. The modification of Plg by adsorbing the CAR not only reduced the volatility of CAR, but means it can also be used as an excellent stabilizer for the emulsions. The size of emulsion droplets decreased with the increase in CAR and Plg content, indicating that a small amount of CAR molecule could play a vital role in modifying the surface characteristics of Plg nanorods and decreasing oil–water interfacial tension (Chen et al., 2019). The modified Plg nanorods adsorbed irreversibly onto the oil–water interface and formed a rigid interfacial film around the oil droplets, which offered an efficient barrier for the coalescence of droplets (Fig. 2i).

CAR Microcapsules Formed by Pickering Emulsion

CAR microcapsules were formed by the electrostatic interaction between HACC and SA and subsequent crosslinking interaction between SA and calcium ions when dropping the Pickering emulsion into the $CaCl_2$ solution. The average diameter of the wet CAR

https://doi.org/10.1007/s42860-022-00200-w Published online by Cambridge University Press

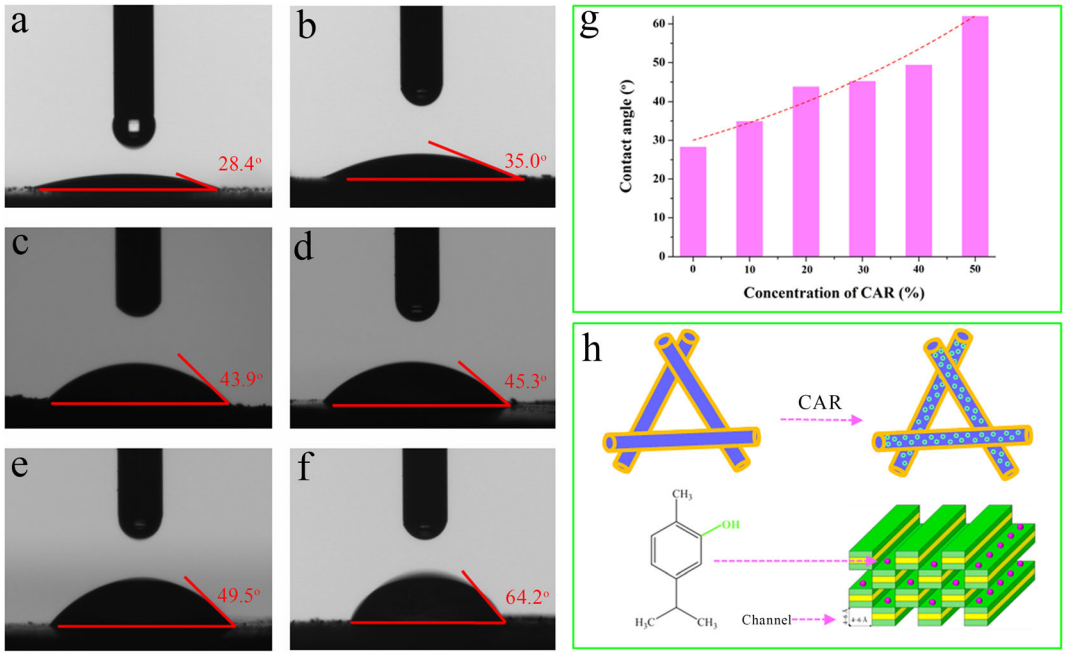

Fig. 1 Contact angle of **a** Plg and Plg mixed with various amounts of **b** 10%, **c** 20%, **d** 30%, **e** 40%, **f** 50% CAR (corresponding to the weight of Plg), **g** the tendency of increasing contact angle with the addition of CAR, and **h** schematic diagram of adsorption interaction between Plg and CAR molecules

microcapsules was 3.5 mm (Fig. 3a). After drying at 37°C, the microcapsules shrank partially; the size reduced from 3.5 to 1.4 mm, and the color changed from white to orange (Fig. 3b, c). Note that the CAR microcapsules have a dense surface but porous interior (Fig. 3c–h) and were formed by the emulsion droplet (Fig. 3f). The SEM images (Fig. 3g–h) showed that the pore diameter of CAR microcapsules was 10–30 μm, and the shell thickness of the pores was ~0.2 μm.

Span 80-stabilized traditional emulsion was also applied to prepare the CAR microcapsules, and the result compared with the microcapsules prepared with Plg stabilized Pickering emulsion is shown in Fig. 4a–c. Obviously, the Pickering emulsion stabilized with modified Plg displayed excellent stability, and the emulsions can be stabilized for 12 months without any creaming or coalescence (Fig. 4c). Conversely, coalescence was observed from the emulsion stabilized with Span 80 at 6 months only (Fig. 4b). Moreover, the emulsions stabilized by Span 80 showed a larger droplet diameter, and the droplet size increased after storage for 12 months (Fig. 4d, e). Meanwhile, the average size of Pickering emulsions stabilized with modified Plg displayed ultra-high stability, and the droplet diameter had only a slight increase from0.5–1 to 1–1.5 μm in 12 months (Fig. 4f, g). The high stability of the Pickering emulsions was attributed to the irreversible adsorption of modified Plg at the oil–water interface (Arab et al., 2018; Binks & Lumsdon, 2000). In addition, the microcapsules obtained from Span 80-stabilized emulsions exhibited poor storability and shrank obviously after drying (Fig. 4h), while the microcapsules obtained from Plg-stabilized Pickering emulsions always remained intact (Fig. 4i).

The formation mechanism of CAR microcapsules was analyzed by FTIR spectroscopy of the Plg (Fig. 5a); the adsorption peak at 1032 cm^{-1} was attributed to the Si–O stretching vibrations of Plg, and at 3440 and 1630 cm^{-1} corresponded to H–O–H of coordinated and zeolitic water of Plg (Blanco et al., 1988; Suárez & García-Romero, 2006). In the spectrum of CAR molecules, the absorption peaks found at 2870, 2962, and 2926 cm^{-1} were assigned to the symmetric and antisymmetric stretching vibration of $–CH_3$ and $–CH_2–$ groups, respectively, and the peak at 3020 cm^{-1} was suggested to be from the C–H stretching vibration of a benzene ring. In addition, the wide absorption bands in the ranges 1422–1586 and 800–900 cm^{-1} were derived from the C=C stretching vibration of aromatic O–H stretching

https://doi.org/10.1007/s42860-022-00200-w Published online by Cambridge University Press

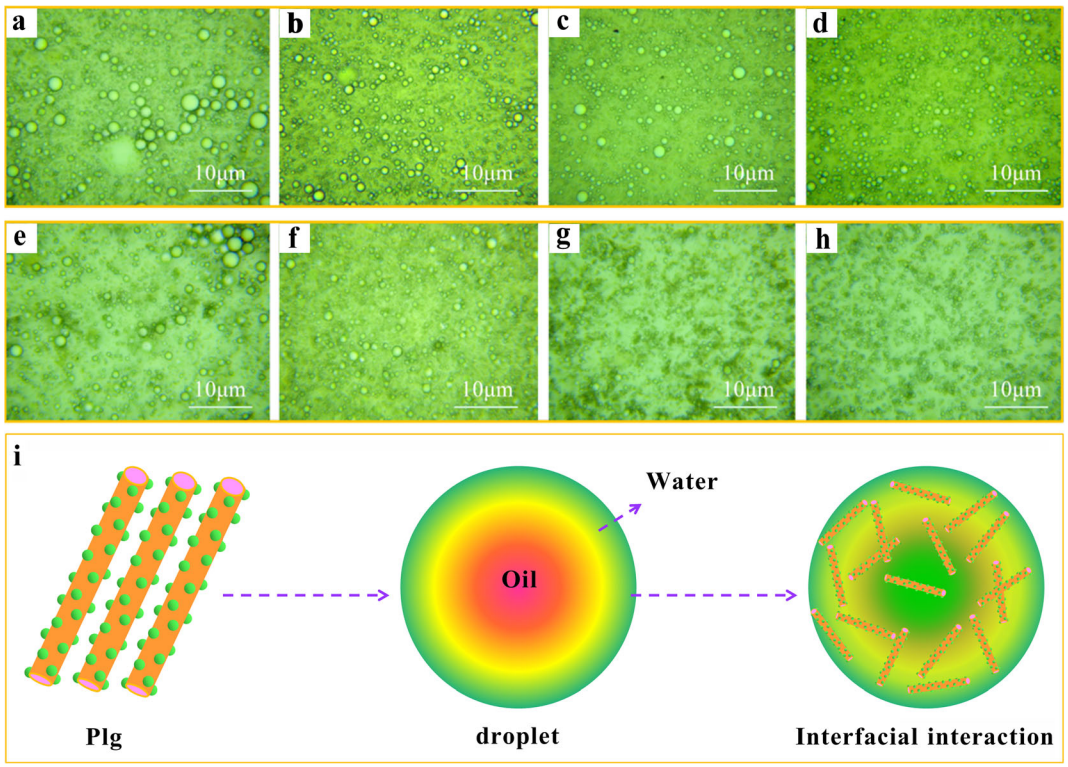

Fig. 2 Optical microscope images of Pickering emulsions with various amounts of Plg: **a** 5%, **b** 10%, **c** 15%, **d** 20% of CAR and 2% Plg, and various amounts of CAR: **e** 4%, **f** 6%, **g** 8%, **h** 10%, and 15% of Plg, and **i** schematic illustration of the interfacial interaction of emulsion droplets

vibrations, and aromatic C–H bending, respectively (Arrieta et al., 2013; Pretsch et al., 2001). With regard to the SA and HACC, the absorption peak at 1625 cm^{-1} in SA was assigned to the stretching vibration of the carboxyl group (Gibson et al., 1999), and peaks at 1487 and 1310 cm^{-1} in HACC were the bending vibration of $–CH_3$ and the stretching vibration of $C–N^+$, respectively (Chen et al., 2016; Manouchehri et al., 2019). When the microcapsules formed, the peaks at 1487 and 1310 cm^{-1} of HACC, as well as 1648 cm^{-1} derived from SA, shifted to 1440, 1248, and 1632 cm^{-1}, respectively, suggesting that the microcapsule shell was built via the electrostatic interactions between quaternary ammonium groups of HACC and the carboxyl groups of SA. The FTIR spectrum of microcapsules containing CAR was the same as the microcapsule shell; a visible difference was in the absorption peaks at 1032 and 996 cm^{-1} which shifted to 1040 and 988 cm^{-1}, possibly due to the interaction between the microcapsule shell and CAR molecules (Fei et al., 2004).

The thermal stability and encapsulation effect of CAR microcapsules prepared by Span 80 stabilized emulsions and Plg-stabilized Pickering emulsions were investigated with TGA and DTG analysis (Fig. 5b). The weight loss of the CAR microcapsules prepared by Span 80-stabilized emulsions also had four stages, which were 50–196, 196–240, 240–360, and 360–750°C. In the DTG curve, the obvious decomposition at 186°C may be attributed to the volatilization and decomposition of the CAR from Plg-stabilized Pickering emulsions, while Span 80-stabilized emulsions appeared at 98°C. The loading content of CAR in the microcapsules prepared from Plg-stabilized Pickering emulsions was also found to be greater than that of the microcapsules formed from Span 80-stabilized conventional emulsion. Meanwhile, the thermal stability of the CAR molecules was improved obviously by the microencapsulation process based on Pickering emulsions. The reason was that the stable Plg particles were incorporated into the matrix of the polymeric network and the stability and strength of microencapsulation were increased, which is indicated by the increased thermostability.

https://doi.org/10.1007/s42860-022-00200-w Published online by Cambridge University Press

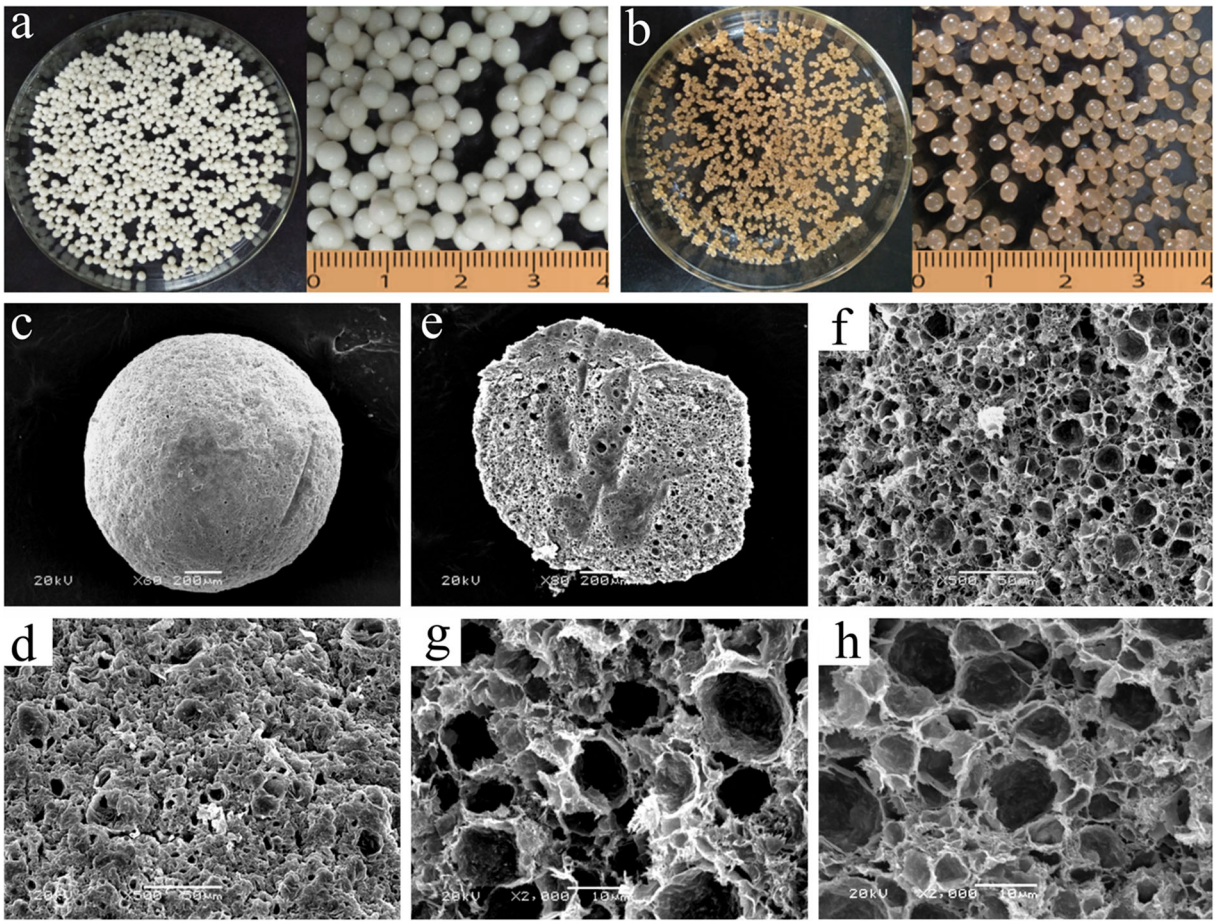

Fig. 3 Digital photographs of: **a** CAR microcapsules prepared by Pickering emulsions formed in aqueous solution (15% of CAR and 8% of Plg); **b** CAR microcapsules after drying at 37°C for 6 h; SEM images of the CAR microcapsules **c**, **d** surface, and **e**, **f**, **g**, **h** cross sections

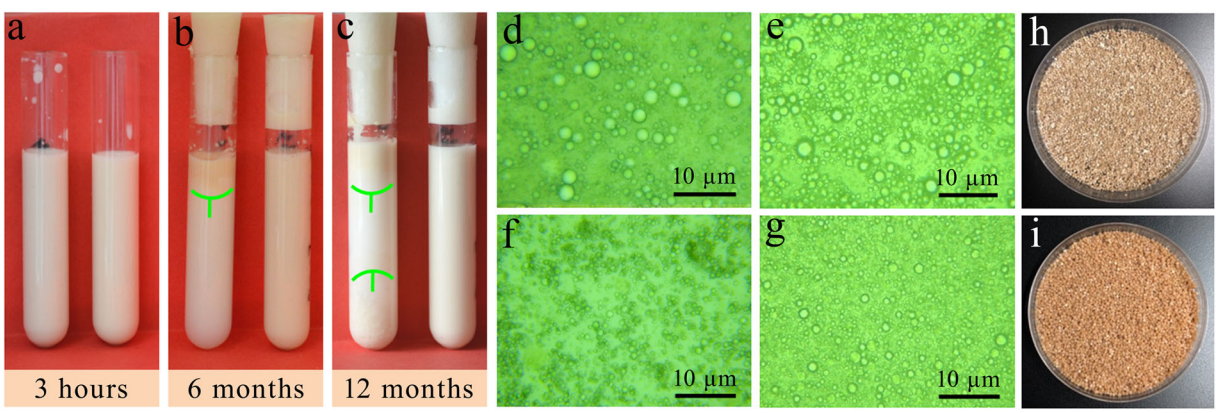

Fig. 4 The emulsions obtained after **a** 3 h, **b** 6 months, **c** 12 months (left tubes are Span 80-stabilized emulsions using 15% CAR and 1% Plg of Span 80; right tubes are Plg-stabilized Pickering emulsions prepared using 15% CAR and 8% Plg, as below). Optical microscopy of Span 80-stabilized emulsions: **d** original emulsions; **e** after 12 months; Plg-stabilized Pickering emulsions: **f** original emulsions; **g** after 12 months. Digital photographs of CAR microcapsules prepared using: **h** Span 80-stabilized emulsions, and **i** Plg-stabilized Pickering emulsions after 12 months

https://doi.org/10.1007/s42860-022-00200-w Published online by Cambridge University Press

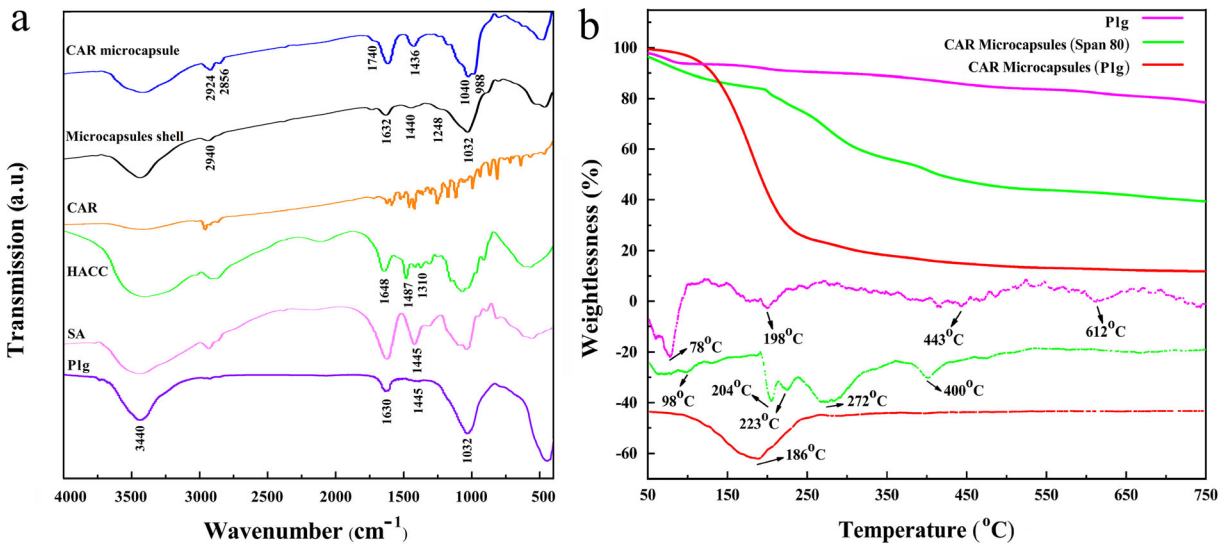

Fig. 5 **a** FTIR spectra of Plg, SA, HACC, CAR, microcapsule shell, and CAR microcapsule prepared using Plg-stabilized Pickering emulsions (15% of CAR and 8% of Plg), and **b** TG and DTGA curves of CAR microcapsule prepared using Span 80-stabilized emulsions (15% CAR and 1% Span 80) and Plg-stabilized Pickering emulsions (15% CAR and 8% Plg)

The optimum conditions of CAR and Plg for the preparation of CAR microcapsules were evaluated by the LC and EE according to the standard curve (Fig. S5), and the results are presented in Table 1. The increase in the CAR content (from 5% to 15% with respect to the weight of the water) resulted in the enhancement of EE (from 40.6% to 56.3%) and LC (from 49.2% to 73.6%). When the CAR content approached 15%, the LC continued to increase, but the EE changed only slightly, indicating that 15% of CAR was the optimal amount for the preparation of CAR microcapsules. With the increase in LC, the CAR in the microcapsules reached saturation, and the EE was enhanced slightly. According to optical microscopy, the addition of Plg reduced the diameter of droplets and also improved the EE. After determining the optimum LC and EE of CAR in microcapsules prepared by Plg-stabilized Pickering emulsions, the next step was to evaluate the antibacterial properties.

Table 1 LC and EE of CAR microcapsules prepared using different amounts of CAR and Plg

Amount of CAR added (%)	Amount of Plg added (%)	LC (%)	EE (%)
5	2	49.2	40.6
10	2	62.0	54.1
15	2	73.6	56.3
20	2	80.5	57.1
15	4	53.1	47.1
15	6	62.4	47.8
15	8	65.5	54.5
15	10	76.5	53.2

Antibacterial Properties

The antibacterial efficacy of the CAR microcapsules was evaluated by counting the growth of colony forming units of model Gram negative and Gram positive bacterial populations compared to the blank (bacteria without treatment) and negative controls (Plg without CAR). CAR microcapsules exhibited various degrees of growth inhibition toward *E. coli* and *S. aureus* (Fig. 6). The blank control groups of *E. coli* and *S. aureus* are also shown in Fig. 6. The bacterial CFU are distributed uniformly in the media, and the microcapsules containing Plg without CAR cannot effectively inhibit growth of Gram negative *E. coli* and Gram positive *S. aureus*. However, microcapsules containing Plg dosed with CAR displayed an increased antibacterial effect on *E. coli* and *S. aureus* with a dose-dependent behavior. *E. coli* and *S. aureus* could be inhibited completely by the microcapsules encapsulated with 15 or 20% of CAR under the same evaluation conditions. The Plg content of CAR

https://doi.org/10.1007/s42860-022-00200-w Published online by Cambridge University Press

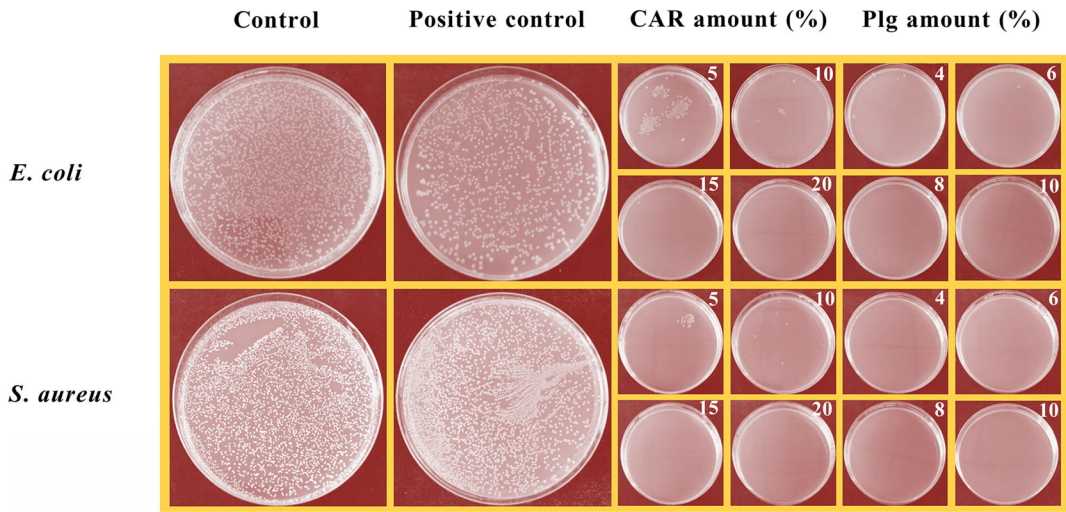

Fig. 6 Photographs of *E. coli* and *S. aureus* colonies cultured after treatment with CAR microcapsules prepared using various amounts of CAR (5%, 10%, 15%, 20% of CAR and 2% of Plg) and Plg (15% of CAR and 4%, 6%, 8%, 10% of Plg)

microcapsules was also a factor affecting the antibacterial activities. Note that 8% of Plg was an appropriate level of additive for reduction of *E. coli* (Fig. 6), while the CAR microcapsules with 6% Plg deactivated *S. aureus* completely. The results indicated that the inhibition rates of the microcapsules were all >98% except for the sample containing 5% CAR (Fig. S6). In addition, *S. aureus* is more sensitive to the CAR microcapsules than *E. coli*. This may be attributed to the enrichment of the *S. aureus* cell membranes in hydrophilic lipopolysaccharides (Liaqat & Eltem, 2018; Shen et al., 2015).

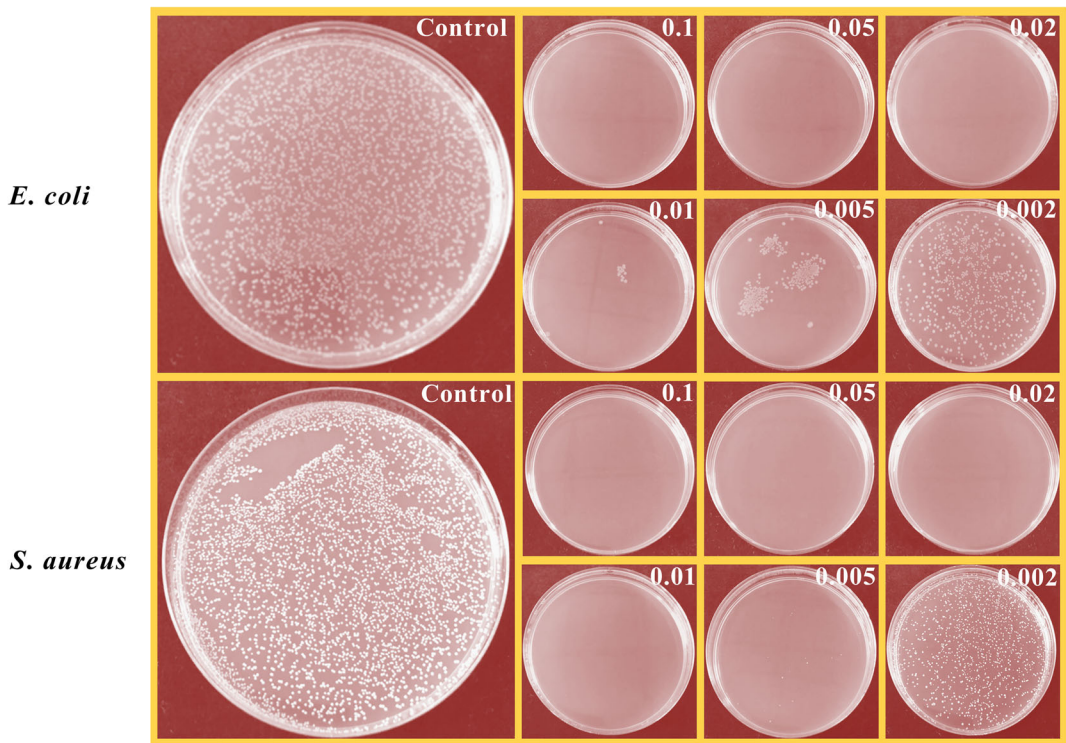

Fig. 7 Quantitative evaluation of the bactericidal effect of various volume percentages of CAR (%) on *E. coli* and *S. aureus*

https://doi.org/10.1007/s42860-022-00200-w Published online by Cambridge University Press

To compare the bactericidal effect of the microcapsules with various amounts of CAR, 'zone of inhibition' experiments for *E. coli* and *S. aureus* were also carried out, as shown in Fig. 7. Compared to the control group, *E. coli* and *S. aureus* were inhibited completely with the volume percentages of CAR in the ranges 0.02–0.1 and 0.005–0.1%, respectively. When the volume percentage of CAR was 0.002%, no obvious difference in the number of bacterial colonies compared to the control group was observed, indicating that this concentration of CAR did not inhibit the growth of *E. coli* or *S. aureus*. Through quantitative evaluation of the antibacterial activity and combining antibacterial efficiency with the effective CAR release, the optimal dosage was determined. Pickering emulsion was beneficial in terms of increasing the water solubility of CAR, but it also reduced the volatility of CAR, thus enhancing the antibacterial activities.

Conclusions

Novel CAR-loaded antibacterial microcapsules were prepared by incorporation of Pickering emulsion technology into the complex coacervation process. The Pickering emulsion was stabilized with Plg modified only by adsorbing the CAR onto the Plg. Then, the microcapsules were formed by electrostatic interaction between SA and HACC and a crosslinking reaction between SA and calcium ions. The CAR microcapsules possessed a nearly sphere-like shape with a mean diameter of 3.5 mm. TG and DTG analysis showed that the CAR microcapsules with Plg had excellent thermal stability. Meanwhile, the CAR microcapsules displayed remarkable antibacterial effects against *E. coli* and *S. aureus*. The inhibition rates toward *E. coli* and *S. aureus* reached 98% when these organisms were treated with 0.02–0.1% and 0.005–0.1% CAR, respectively. The CAR microcapsules prepared in this study may be used as antibacterial agents in food preservatives, animal feed, and other health-related consumer products.

Supplementary Information The online version contains supplementary material available at https://doi.org/10.1007/s42860-022-00200-w.

Acknowledgments This work was supported financially by the Natural Science Foundation of China (22105212), the Natural Science Foundation of Gansu, China (21JR7RA079), and the Regional Key Project of the Science and Technology Service of the Chinese Academy of Sciences (KFJ-STS-QYZX-086).

Authors' Contributions Aiping Hui: Manuscript writing, experimental design, data analysis and data collection.

Yongfeng Zhu: Manuscript review, data analysis and data collection.

Fangfang Yang, Yuru Kang: Data analysis and data collection.

Aiqin Wang: Manuscript review, experimental design.

Funding Funding sources are as stated in the Acknowledgments.

Data Availability The datasets generated during the current study are available from the corresponding author on reasonable request.Supplementary Information The online version contains supplementary material available at https://doi.org/10.1007/s42860-022-00200-w.

Declarations

Conflict of Interest The authors declare that they have no conflict of interest.

Consent for Publication N/A.

References

Alkan Tas, B., Sehit, E., Erdinc Tas, C., Unal, S., Cebeci, F. C., Menceloglu, Y. Z., & Unal, H. (2019). Carvacrol loaded halloysite coatings for antimicrobial food packaging applications. *Food Packaging and Shelf Life, 20*, 100300.

Arab, D., Kantzas, A., & Bryant, S. L. (2018). Nanoparticle stabilized oil in water emulsions: A critical review. *Journal of Petroleum Science and Engineering, 163*, 217–242.

Arrieta, M. P., Peltzer, M. A., Garrigós, M. D. C., & Jiménez, A. (2013). Structure and mechanical properties of sodium and calcium caseinate edible active films with carvacrol. *Journal of Food Engineering, 114*, 486–494.

Bahrami, A., Delshadi, R., Assadpour, E., Jafari, S. M., & Williams, L. (2020). Antimicrobial-loaded nanocarriers for food packaging applications. *Advances in Colloid and Interface Science, 278*, 102140.

Bakry, A. M., Huang, J. J., Zhai, Y. Y., & Huang, Q. L. (2019). Myofibrillar protein with κ- or λ-carrageenans as novel shell materials for microencapsulation of tuna oil through complex coacervation. *Food Hydrocolloids, 96*, 43–53.

Binks, B. P., & Lumsdon, S. O. (2000). Influence of particle wettability on the type and stability of surfactant-free emulsions. *Langmuir, 16*, 8622–8631.

Blanco, C., Herrero, J., Mendioroz, S., & Pajares, J. A. (1988). Infrared studies of surface acidity and reversible folding in palygorskite. *Clay and Clay Minerals, 36*, 364–368.

Cai, X. L., Li, C. J., Tang, Q., Zhen, B. W., Xie, X. L., Zhu, W. F., Zhou, C. H., & Wang, L. J. (2019). Assembling kaolinite

nanotube at water/oil interface for enhancing Pickering emulsion stability. *Applied Clay Science, 172*, 115–122.

Chen, D. F., Wang, A. Q., Li, Y. M., Hou, Y. J., & Wang, Z. N. (2019). Biosurfactant-modified palygorskite clay as solid-stabilizers for effective oil spill dispersion. *Chemosphere, 226*, 1–7.

Chen, M. J., Hu, Y., Zhou, J., Xie, Y. R., Wu, H., Yuan, T., & Yang, Z. H. (2016). Facile fabrication of tea tree oil-loaded antibacterial microcapsules by complex coacervation of sodium alginate/quaternary ammonium salt of chitosan. *RSC Advances, 6*, 13032–13039.

Chuesiang, P., Sanguandeekul, R., & Siripatrawan, U. (2021). Enhancing effect of nanoemulsion on antimicrobial activity of cinnamon essential oil against foodborne pathogens in refrigerated Asian seabass (*Lates calcarifer*) fillets. *Food Control, 122*, 107782.

Dong, Z. J., Ma, Y., Hayat, K., Jia, C. S., Xia, S. Q., & Zhang, X. M. (2011). Morphology and release profile of microcapsules encapsulating peppermint oil by complex coacervation. *Journal of Food Engineering, 104*, 455–460.

Fei, B., Chen, C., Peng, S., Zhao, X., Wang, X., & Dong, L. (2004). FTIR study of poly (propylene carbonate)/bisphenol A blends. *Polymer International, 53*, 2092–2098.

Gibson, D. H., Ding, Y., Miller, R. L., Sleadd, B. A., Mashuta, M. S., & Richardson, J. F. (1999). Synthesis and characterization of ruthenium, rhenium and titanium formate, acetate and trifluoroacetate complexes. Correlation of IR spectral properties and bonding types. *Polyhedron, 18*, 1189–1200.

Hui, A. P., Yan, R., Wang, W. B., Wang, Q., Zhou, Y. M., & Wang, A. Q. (2020). Incorporation of quaternary ammonium chitooligosaccharides on ZnO/palygorskite nanocomposites for enhancing antibacterial activities. *Carbohydrate Polymers, 247*, 116685.

Issouffou, C., Suwansri, S., Salaipeth, L., Domig, K. J., & Hwanhlem, N. (2018). Synergistic effect of essential oils and enterocin KT2.W2G on the growth of spoilage microorganisms isolated from spoiled banana peel. *Food Control, 89*, 260–269.

Kang, Y. R., Mu, B., Zhu, G., Zhu, Y. F., & Wang, A. Q. (2022). Preparation and properties of antibacterial polyhexamethylene biguanide/palygorskite composites as zearalenone adsorbents. *Clay and Clay Minerals, 70*, 182–195.

Kretz, R. (1983). Symbols for rock-forming minerals. *American Mineralogist, 68*, 277–279.

Li, S. E., Mu, B., Ding, J. J., Zhang, H., Wang, X. W., & Wang, A. Q. (2021a). Fabrication of anthocyanin/montmorillonite hybrid pigments for enhancing environmental stabilities and application composite films. *Clays and Clay Minerals, 69*, 142–151.

Li, Y. C., Zhao, R., Hu, F. H., Lu, P., Ji, D. D., Luo, Q., Li, G. D., Yu, D. H., Wang, H. L., Song, Z. P., Li, S., & Liu, W. X. (2021b). Laponite/lauric arginate stabilized AKD Pickering emulsions with shell-tunable hydrolytic resistance for use in sizing paper. *Applied Clay Science, 206*, 106085.

Liaqat, F., & Eltem, R. (2018). Chitooligosaccharides and their biological activities: A comprehensive review. *Carbohydrate Polymers, 184*, 243–259.

Lu, J., Tian, X. X., Jin, Y. L., Chen, J., Walters, K. B., & Ding, S. J. (2014). A pH responsive Pickering emulsion stabilized by fibrous palygorskite particles. *Applied Clay Science, 102*, 113–120.

Lu, T. T., Zhu, Y. F., Wang, W. B., & Wang, A. Q. (2020). Controllable fabrication of hierarchically porous adsorbent via natural particles stabilized Pickering medium internal phase emulsion for high-efficiency removal of Rb^+ and Cs^+. *Journal of Cleaner Production, 277*, 124092.

Ma, J. Z., Liu, J. L., Bao, Y., Zhu, Z. F., Wang, X. F., & Zhang, J. (2013). Synthesis of large-scale uniform mulberry-like ZnO particles with microwave hydrothermal method and its antibacterial property. *Ceramics International, 39*, 2803–2810.

Manouchehri, F., Sadeghi, B., Najaf, F., Mosslemin, M. H., & Niakan, M. (2019). Synthesis and characterization of novel polymerizable bis quaternary ammonium dimethacrylate monomers with antibacterial activity as an efficient adhesive system for dental restoration. *Polymer Bulletin, 76*, 1295–1315.

Marosz, M., Kowalczyk, A., Gil, B., & Chmielarzet, L. (2020). Acid-treated clay minerals as catalysts for dehydration of methanol and ethanol. *Clays and Clay Minerals, 68*, 23–37.

Muhoza, B., Xia, S. Q., Cai, J. B., Zhang, X. M., Duhoranimana, E., & Sub, J. K. (2019). Gelatin and pectin complex coacervates as carriers for cinnamaldehyde: Effect of pectin esterification degree on coacervate formation, and enhanced thermal stability. *Food Hydrocolloids, 87*, 712–722.

Pan, C., & Liu, P. (2021). Amphiphilic polymer-grafted palygorskite nanorods via surface olefin cross-metathesis for versatile applications. *Applied Clay Science, 200*, 105889.

Pickering, S. U. (1907). Emulsions. *Journal of the Chemical Society, Transactions, 91*, 2001–2021.

Ramsden, W. (1903). Separation of solids in the surface-layers of solutions and 'suspensions'. *Proceedings of the Royal Society of London, 72*, 156–164.

Pretsch, E., Bühlmann, P., Affolter, C., Herrera, A., & Martínez, R. (2001). *Determinación estructural de compuestos orgánicos*. Springer-Verlag Ibérica.

Ryu, V., Corradini, M. G., Mc Clements, D. J., & Mc Landsborough, L. (2019). Impact of ripening inhibitors on molecular transport of antimicrobial components from essential oil nanoemulsions. *Journal of Colloid Interface Science, 556*, 568–576.

Sharifi-Rad, M., Varoni, E. M., Iriti, M., Martorell, M., Setzer, W. N., del Mar Contreras, M., Salehi, B., Soltani-Nejad, A., Rajabi, S., Tajbakhsh, M., & Sharifi-Rad, J. (2018). Carvacrol and human health: A comprehensive review. *Phytotherapy Research, 32*, 1675–1687.

Shen, S. X., Zhang, T. H., Yuan, Y., Lin, S. Y., Xu, J. Y., & Ye, H. Q. (2015). Effects of cinnamaldehyde on *Escherichia coli*, and *Staphylococcus aureus* membrane. *Food Control, 47*, 196–202.

Shi, C., Zhang, X., & Gu, N. (2018). The antimicrobial activities and action-mechanism of tea tree oil against food-borne bacteria in fresh cucumber juice. *Microbial Pathogenesis, 125*, 262–271.

Suárez, M., & García-Romero, E. (2006). FTIR spectroscopic study of palygorskite: Influence of the composition of the octahedral sheet. *Applied Clay Science, 31*, 154–163.

Tariq, S., Wani, S., Rasool, W., Shafi, K., Bhat, M. A., Prabhakar, A., Shalla, A. H., & Rather, M. A. (2019). A comprehensive review of the antibacterial, antifungal and antiviral potential of essential oils and their chemical constituents against drug-

resistant microbial pathogens. *Microbial Pathogenesis, 134*, 103580.

Timilsena, Y. P., Wang, B., Adhikari, R., & Adhikari, B. (2017). Advances in microencapsulation of polyunsaturated fatty acids (PUFAs)-rich plant oils using complex coacervation: A review. *Food Hydrocolloids, 69*, 369–381.

Vel, E. V. D., Sampers, I., & Raes, K. (2017). A review on influencing factors on the minimum inhibitory concentration of essential oils. *Critical Reviews in Food Science and Nutrition, 58*, 1–22.

Wang, S. J., Shen, Y., Chen, X. P., Dong, L. M., Yu, H., Bao, M. T., & Li, Y. M. (2022). Cationic surfactant-modified palygorskite particles as effective stabilizer for Pickering emulsion gel formation. *Applied Clay Science, 219*, 106439.

Wang, W. B., Tian, G. Y., Zhang, Z. F., & Wang, A. Q. (2015). A simple hydrothermal approach to modify palygorskite for high-efficient adsorption of Methylene blue and Cu(II) ions. *Chemical Engineering Journal, 265*, 228–238.

Yang, X., Gao, N., Hu, L. D., Li, J. L., & Sun, Y. B. (2015). Development and evaluation of novel microcapsules containing poppy-seed oil using complex coacervation. *Journal of Food Engineering, 161*, 87–93.

Yang, Z. M., Peng, Z., Li, J. H., Li, S. D., Kong, L. X., Li, P. W., & Wang, Q. H. (2014). Development and evaluation of novel flavour microcapsules containing vanilla oil using complex coacervation approach. *Food Chemistry, 145*, 272–277.

Yildiz, Z. I., Celebioglu, A., Kilic, M. E., Durgun, E., & Uyar, T. (2018). Fast-dissolving carvacrol/cyclodextrin inclusion complex electrospun fibers with enhanced thermal stability, water solubility, and antioxidant activity. *Journal of Materials Science, 53*, 15837–15849.

Yin, H. B., Chen, C. H., Kollanoor-Johny, A., Darre, M. J., & Venkitanarayanan, K. (2015). Controlling *Aspergillus flavus* and *Aspergillus parasiticus* growth and aflatoxin production in poultry feed using carvacrol and trans-cinnamaldehyde. *Poultry Science, 94*, 2183–2190.

Zhong, H. Q., Mu, B., Zhang, M. M., Hui, A. P., Kang, Y. R., & Wang, A. Q. (2020). Preparation of effective carvacrol/attapulgite hybrid antibacterial materials by mechanical milling. *Journal of Porous Materials, 27*, 843–853.

Zhong, H. Q., Mu, B., Yan, P. J., Jing, Y. M., Hui, A. P., & Wang, A. Q. (2021). A comparative study on surface/interface mechanism and antibacterial properties of different hybrid materials prepared with essential oils active ingredients and palygorskite. *Colloids and Surfaces A: Physicochemical and Engineering Aspects, 618*, 126455.

https://doi.org/10.1007/s42860-022-00200-w Published online by Cambridge University Press